Environmental Science and Pollution Research
https://doi.org/10.1007/s11356-020-08922-x

RESEARCH ARTICLE

Aluminum leaching from water treatment sludge using hydrochloric acid and kinetic study

Agus Mirwan[1] · Meilana Dharma Putra[1] · Jhy-Chern Liu[2] · Susianto[3] · Ali Altway[3] · Renanto Handogo[3]

Received: 24 December 2019 / Accepted: 16 April 2020

Abstract

Water treatment sludge (WTS) is abundantly produced in the world; the waste contributes to the environmental problems. Therefore, for WTS utilization, aluminum leaching was employed using hydrochloric acid in this study. Al leaching efficiency increased from 72% to 80% as hydrochloric acid concentration increased from 1 to 4 M. Decreasing the particle size and increasing the temperature increased Al leaching efficiency. The proposed kinetic model revealed that the rate-controlling step followed a series of two leaching mechanisms: initially controlled by product-layer diffusion and then by a chemically controlled reaction. For instance, at 70 °C, the initial stage is well fitted by product-layer diffusion ($R^2 = 0.87$) compared to $R^2 = 0.60$ for chemical reaction; while for the second stage, $R^2 = 0.95$ was observed via chemical reaction compared to $R^2 = 0.74$ for product-layer diffusion. The activation energies in these two stages were 9.58 kJ/mol and 10.73 kJ/mol, respectively. The proposed model was well validated by using data from literature and thus will be useful for other applications of leaching and extraction processes.

Keywords Waste · Environmental problem · Mechanism · Model · Chemical surface · Diffusion · Removal

Introduction

Water treatment plants (WTP) involve a coagulation process by using aluminum salts, e.g., polyaluminum chloride or aluminum sulfate, that cause hydrolyzation in raw water to form aluminum hydroxide precipitates. This process results in the production of voluminous sludge known as WTS. Globally, the total production of WTS can reach 10,000 tons/day (Okuda et al. 2014). Being a non-toxic material, most of WTS is disposed for land application and landfilling (Babatunde and Zhao 2007; Nair and Ahammed 2015). On the other hand, recycling WTS should be avoided because of organic solubilization (Meng et al. 2018). In recent years, many studies have been focused on Al recovery from WTS by leaching processes for possible reuse (Haynes and Zhou 2015). Various methods such as acidification, basification, ion exchange, and membranes have been employed for the recovery (Ahmad et al. 2016b; Nair and Ahammed 2014; Ooi et al. 2018). Ahmad et al. (2016a) indicated that Al recovery might not be simple, even though laboratory and plant scale tests have showed that it is feasible and economical. Intensive research in acid leaching has been under development due to the efficient and low-cost process compared to other methods (Jiménez et al. 2007). Thus, further exploration of means to recover Al from WTS is deemed important.

Acids have been examined for Al leaching from WTS. The commonly used sulfuric acid (H_2SO_4) is one of the effective solvents to extract aluminum. Jiménez et al. (Xu et al. 2009) reported that sulfuric acid could extract 70% of Al within 30 min at pH = 2. The leaching efficiency of Al reached 83.6% using 1 M H_2SO_4 within 30 min (Cui et al. 2015). Okuda et al. (Okuda et al. 2014) reported that more than 80% of Al was extracted within 2 h using H_2SO_4 at pH = 1 under ambient temperature. However, due to its toxicity, sulfuric acid can bring some negative effects on environment and could lead to self-inhibition effect due to the new interaction during leaching process (Seidel and Zimmels 1998). The use

Responsible editor: Ta Yeong Wu

✉ Meilana Dharma Putra
mdputra@ulm.ac.id

[1] Department of Chemical Engineering, Faculty of Engineering, Lambung Mangkurat University, Banjarbaru 70714, Indonesia

[2] Department of Chemical Engineering, National Taiwan University of Science and Technology, Taipei 106, Taiwan

[3] Department of Chemical Engineering, Faculty of Industrial Technology, Institut Teknologi Sepuluh Nopember, Surabaya 60111, Indonesia

Published online: 29 April 2020

of hydrochloric acid as a solvent in leaching is gaining grounds in research due to its lower acute toxicity compared to sulfuric acid (Hagen and Järnberg 2009). The leaching process using HCl continues to improve to attain high efficiency. It was reported that the sulfuric acid and hydrochloric acid lead to corrosion effect in vessel; however, corrosion rate for both acid can be significantly reduced by using hard chrome plating (Ajeel et al. 2012). The leaching rate of Al from secondary aluminum dross at 75 °C for 600 min was about 7–18% (Yang et al. 2019a). On the other hand, the extraction efficiency of 94% was obtained from raw kaolin using HCl at 70 °C for 6 h; however, sodium chloride was also formed (Bhattacharyya and Behera 2017). The leaching efficiency using HCl varied depending on the raw materials and process condition such as temperature and time.

Kinetic models are important tools to describe the mechanism of the leaching process. Some studies have used the shrinking core model to define the dissolution kinetics of aluminum from fly ash and kaolin (Cheng et al. 2012; Tang et al. 2010). A kinetic process of aluminum leaching is described via diffusion or chemical reaction. However, the exact rate-limiting step for the kinetics is still undetermined for a general aluminum leaching process. Hence, the kinetics should be studied in detail to explore the role of the rate-limiting step in the system.

Many studies have been devoted to assess the optimal conditions for acid leaching of Al from the WTS. However, most of them were focused on the use of H_2SO_4 (Cheng et al. 2016; Cheng et al. 2012; Keeley et al. 2016). Some leaching processes have been also carried out from raw materials using HCl; thus, the Al leaching process from WTS using HCl would be investigated thoroughly in this study. On the other hand, the information on the mechanism of leaching process seems insufficient. In the present study, the effects of some main parameters, such as acid concentration, particle size, and temperature on Al leaching have been investigated using HCl. The kinetics of Al leaching from WTS has been further studied using the shrinking core (SC) model. A modified kinetic model has also been developed in this study.

Material and methods

Materials and characterization

WTS was collected from the water treatment plant in Banjarmasin, South Kalimantan, Indonesia. It was washed and dried under direct sunlight for 48 h. The material was further crushed, screened, and separated into the size fractions of 70–120 mesh (0.210–0.125 mm), 120–200 mesh (0.125–0.074 mm), and 200–325 mesh (0.074–0.044 mm). Samples were then stored in plastic bottles for experiments without any further treatment.

WTS was characterized by X-ray diffractometer (XRD, Philips X-pert powder model, Netherlands) using powder diffraction database file-2 (PDF-2). The results showed the major mineral phases of kaolinite ($Al_2Si_2O_5(OH)_4$), quartz (SiO_2), hematite (Fe_2O_3), and corundum (Al_2O_3) (Fig. 1). The surface functional groups of each constituent solids were characterized using Fourier Transformation Infrared Spectroscopy (FTIR, Shimadzu, Japan), and the results of which are shown in Table 1. Flake structure of WTS was found when being analyzed by scanning electron microscopy equipped with X-ray microanalysis (SEM-EDX, SEM EVO MA 10, Germany). The results showed the presence of dominant elements, namely Al, Si, and Fe (color difference) with the composition of 32.78%, 49.15%, and 18.07%, respectively, as shown in Fig. 2. A similar observation of WTS sample was also shown in other literatures containing Fe_2O_3, SiO_2, and Al_2O_3 (Ahmad et al. 2016b; Cheng et al. 2012).

Aluminum content in the samples was determined by using the inductively coupled plasmacluster optical emission spectrometer (ICP-OES, 9060-D Teledyne Leeman Labs, USA). Each analysis was triplicated and the average value was reported. The Al leaching ratio (x) can be calculated as:

$$x = X/X_0 \tag{1}$$

where X_0 denotes total Al content and X refers to the amount of Al leached (Yang et al. 2019b).

Leaching process

The leaching process was conducted in a 500-mL Pyrex reactor with a thermostat water bath (Fig. 3). Mixing was achieved by using a magnetic stirrer at 300 rpm. Al leaching from WTS was carried out by placing 5 g of WTS into 250 ml of HCl (37%, Sigma-Aldrich) solution at various concentrations (1, 2, 4, and 6 M). WTS samples with different particle sizes (70–120, 120–200, and 200–325 mesh) were used in experiments

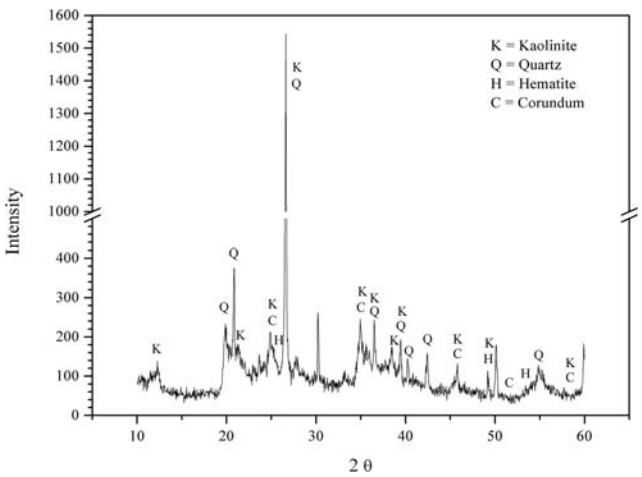

Fig. 1 XRD pattern of WTS

Table 1 Surface functional groups of FTIR of WTS

Infrared band (cm^{-1})	Transmittance (%)	Functional group
3695.36	29.586	Al–O–H str (kaolinite, illite)
3620.14	26.456	Al–O–H (kaolinite, illite, calcite)
3448.49	24.903	H–O–H str (kaolinite, illite)
1634.56	37.454	H–O–H str (illite, calcite)
1104.17	16.372	Si–O str (kaolinite, quartz)
1031.85	8.981	Si–O–Si, Si–O str. (kaolinite, illite)
1007.74	10.150	Si–O str (kaolinite, quartz)
913.23	23.281	Al–O–H str (kaolinite, illite, hematite)
779.19	32.612	Si–O–Al str (kaolinite, illite)
694.33	29.459	Si–O str, Si–O–Al str (quartz, kaolinite)
536.17	15.456	Si–O str, Si–O–Al str (kaolinite)
468.67	13.958	Si–O str, Si–O–Fe str. (quartz, kaolinite)
426.24	21.678	Si–O str (quartz)

conducted at different reaction temperatures (30, 50, 70, and 90 °C). Total reaction time was controlled at 60 min. At selected time interval, samples were collected and then filtered by a syringe for the analysis of Al content.

Shrinking core (SC) model

The shrinking core (SC) model describes the kinetic characteristics of non-catalytic, heterogeneous, solid-liquid reactions consisting of three processes: film diffusion, product-layer diffusion, and surface chemical reaction (Keeley et al. 2016). In this study, only product-layer diffusion and surface chemical reaction were considered due to the fast process of film diffusion. The kinetic equation for a leaching process controlled by a surface chemical reaction is presented as follows:

$$\frac{t}{\tau_c} = 1(1-x)^{1/3} \tag{2}$$

If the leaching process is controlled by the diffusion through product-layer, the kinetic equation is described as follows:

$$\frac{t}{\tau_i} = 1-3(1-x)^{2/3} + 2(1-x) \tag{3}$$

where τ_c is the complete leaching time for process controlled by surface chemical reaction, $\tau_c = \rho_B R/bM_w k_c C_A$, τ_i is the complete leaching time for a process controlled by product-

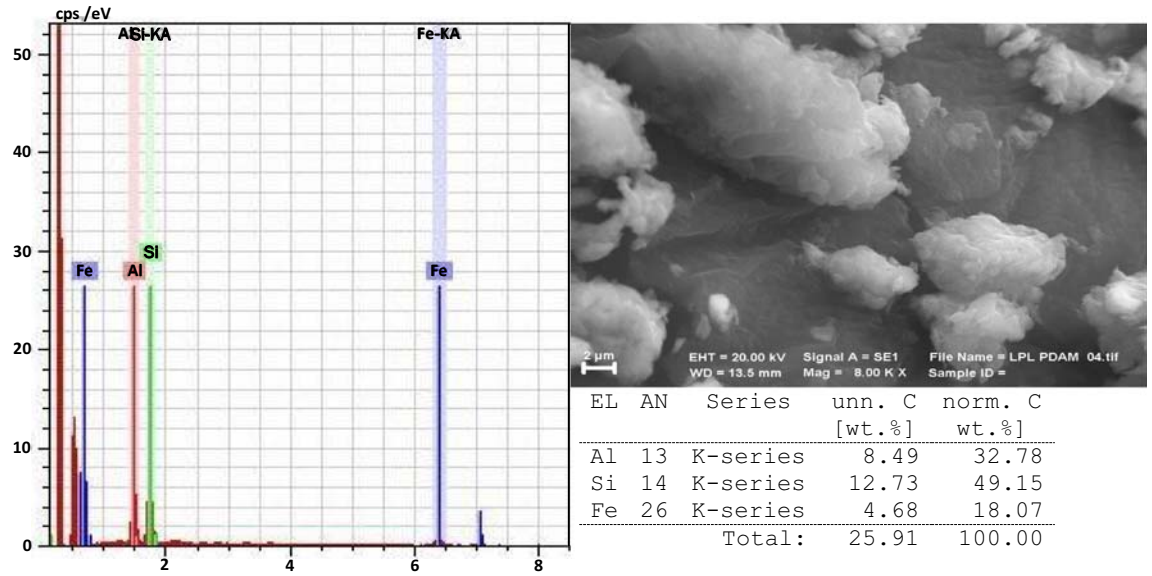

Fig. 2 SEM pictures of WTS

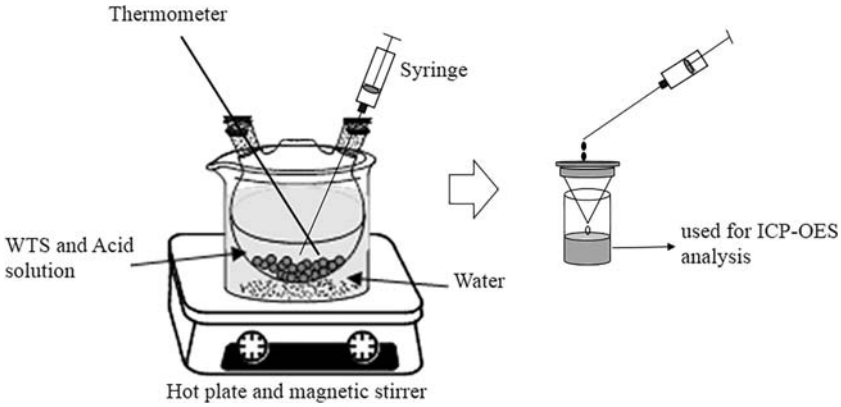

Fig. 3 Leaching process and equipment

layer diffusion, $\tau_i = \rho_B R^2/6bM_w D_e C_A$, x is the fraction of Al leached out, t is the reaction time, ρ_B is the solid density, R is the radius of initial particle, b is the stoichiometric coefficient, M_w is the molecular weight (g/mol), k_c is the factor of mass transfer, C_A is the hydrochloric acid concentration, and D_e is the coefficient of product-layer diffusion.

Results and discussion

Effect of acid concentration

Figure 4 shows the amount of extracted aluminum with time at the temperature of 90 °C, particle size of 200–325 mesh and various concentrations. Aluminum (Al) is the major element of the WTS in the form of $Al(OH)_3$ and the solubility is affected by pH. The main reaction in the leaching process is shown as follows:

$$Al(OH)_{3(s)} + 3HCI_{(aq)} \rightarrow AlCl_{3(aq)} + 3H_2O.$$

As shown in Fig. 4, the efficiency of Al leaching increased from 72% to 80% as HCl concentration changed from 1 to 4 M. Although at 6 M of HCl, it slightly decreased to 78% indicating the key role the pH plays in Al leaching from WTS. This acidification process (with low pH) is more convenient and efficient compared to the basification process (Baba et al. 2009). As reported by Cheng et al. (Cheng et al. 2012), metal such as Al is easily dissolved at pH < 2.5. On the other hand, the solubility of aluminum chloride ($AlCl_3$) decreases with increasing HCl concentration at concentration higher than 5 M (Seidel and Zimmels 1998); this notion is similarly in accordance with our finding here (> 4 M). It was plausible due to the formation of other metal-chloride (Raza et al. 2015). When $AlCl_3$ is saturated in the reaction system, dissolution and precipitation of $Al(OH)_3$ might reach a dynamic equilibrium. The HCl concentration of 4 M was therefore chosen for subsequent experiments.

Effect of particle size and temperature

Figure 5 shows the amount of extracted aluminum with time at the concentration of 4 M, at the temperature of 90 °C and with various particle sizes. The efficiency of Al leaching increased as particle size decreased. It indicated that smaller particle sizes lead to faster leaching process. It could be reasonably

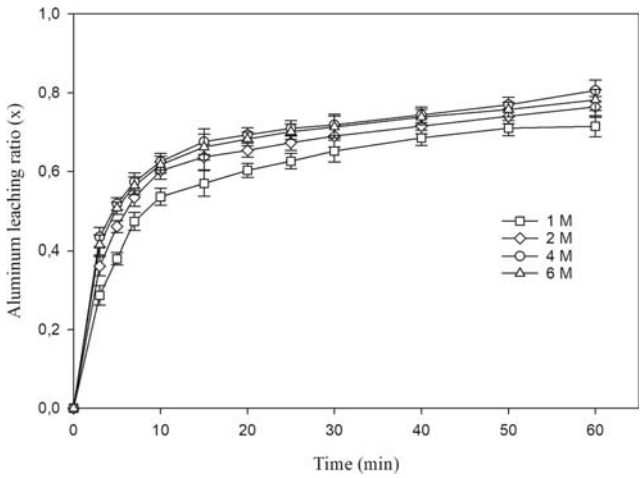

Fig. 4 Effect of acid concentration on Al leaching from WTS

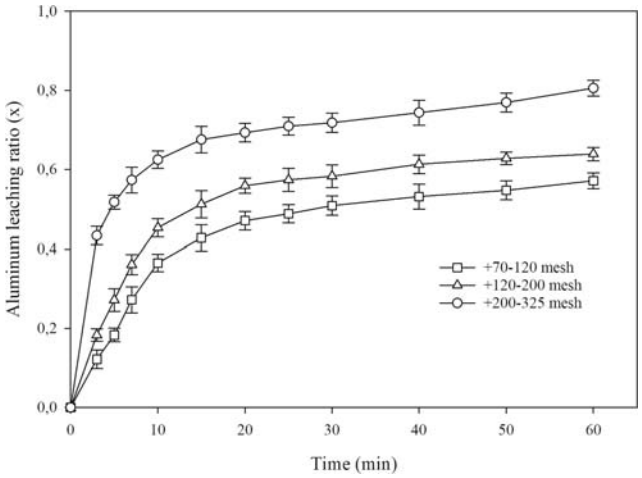

Fig. 5 Effect of particle size on Al leaching from WTS

related to the acceleration of the mass transfer process (Brantley et al. 2008) thus minimizing the effect of internal diffusion. Also, smaller particle size increased the surface area; thus, it consequently resulted in larger contact between particle and solvent (Adekola et al. 2017). Figure 6 shows the amount of extracted aluminum with time at acid concentration of 4 M, particle size of 200–325 mesh, and various temperatures. The Al leaching efficiency increased with temperature and an optimum process was obtained at 4 M and 90 °C for 60 min with the efficiency of 82%. Increasing the temperature from 70 to 90 °C significantly increased the Al leaching efficiency (from 67% to 82%) compared with the increasing temperature from 50 to 70 °C (62% to 67%) and from 30 to 50 °C (58% to 62%). This revealed that the temperature range 70–90 °C is crucial for the leaching process; this situation will plausibly continue at a higher temperature. Significantly higher leaching efficiency (> 70%) was observed by increasing temperature at above 70 °C (Raza et al. 2015; Shalchian et al. 2018). On the other hand, a leaching efficiency of about 99% was obtained at 70 °C using succinic acid, an expensive solvent (Raza et al. 2015). The different results could be attributed to differences in used solvents and extracted components.

Statistical analysis

The resulted data were also affirmed by conducting statistical test using ANOVA analysis. Significant effect of HCl concentration on the Al leaching ratio ($p = 0.0007$) was obtained. Significant effect were also obtained in each range of concentration between 1 and 2 M ($p = 0.0474$), 2 and 4 M ($p = 0.0343$); while insignificant effect was observed in the concentration range of 4 M and 6 M ($p = 0.2924$) due to the drop of Al leaching ratio at higher concentration.

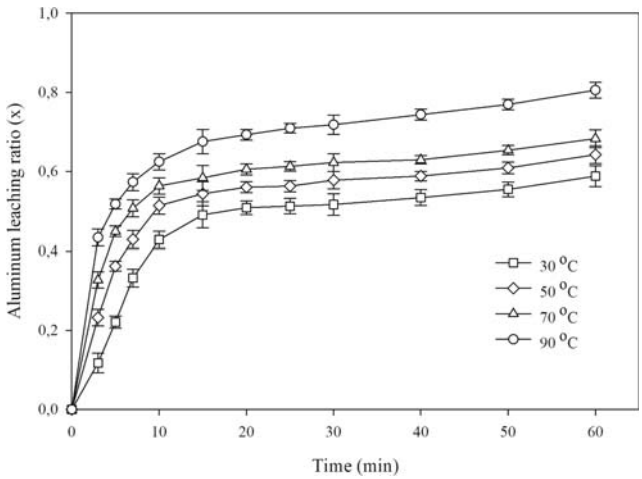

Fig. 6 Effect of temperatures on Al leaching from WTS

For size particle effect, significant effect was also achieved at total range ($p = 1.57 \times 10^{-7}$) as well as in each range between + 70/− 120 and + 120/− 200 ($p = 0.0027$) and + 120/− 200 and + 200/− 325 ($p = 6.84 \times 10^{-5}$). The statistical results also revealed the significant effect of temperature on Al leaching ratio at total temperature range ($p = 1.29 \times 10^{-8}$) and the range of 30 °C and 50 °C ($p = 0.0124$), 50 °C and 70 °C ($p = 0.0284$), and 70 °C and 90 °C ($p = 0.0005$).

Kinetic study and mechanism

Kinetic study is important to elucidate the various processes in the system. The shrinking core model used in the study includes the product-layer diffusion and chemical reaction. The kinetic model using shrinking model has been applied to fit the experimental data. The correlation coefficient values (R^2) for product-layer diffusion and chemical reaction were 0.75–0.84 and 0.57–0.67, respectively, for all experimental data of concentration, particle size, and temperature. Although the fitting results of the kinetic model and experimental were unsatisfactory, the product-layer diffusion as a rate-limiting step was found more appropriate for the system. It was reported that for the process controlled by surface chemical reaction, a plot of $1-(1-x)^{1/3}$ should be a straight line with slope of $1/\tau_c$ and for the process controlled by the product-layer diffusion, a plot of $1-3(1-x)^{2/3}+2(1-x)$ should be a straight line with slope of $1/\tau_i$ (Tian et al. 2018; Yang et al. 2019b, 2020). However, the low values of R^2 obtained here were, probably, because both the exponential rate and linear rate were observed in the leaching process thereby it could not be tackled by the shrinking model. On other hand, the chemical reaction controlled the kinetic process (Brantley et al. 2008); contrarily, the kinetic model of product-layer diffusion was proven to fit the experimental data (Cheng et al. 2012). Those different results of the rate of limiting step were due to the used solvent, the extracted component, the raw materials, and the temperature affecting the kinetic process (Brantley et al. 2008). In fact, the kinetic model in those literatures was only evaluated during the exponential rate of leaching, while the subsequent leaching rate cannot be ignored as the increase in the leaching efficiency was observed at about 14–20% (Cui et al. 2015). On the other hand, researchers revealed that the experimental data did not conform to both kinetic models of chemical reaction or product-layer diffusion (Yang et al. 2019b); they concluded that the mathematical approach failed to explain the dynamic situation due to finer particle size, grain shape, and reactant activity (Shalchian et al. 2018). In fact, they had both stages of exponential and linear leaching process. Hence, their difficulty of interpretation can be clearly described in this study later. In the next discussion, we will clearly explore the effect of product-layer diffusion and chemical reaction as rate-limiting step on both proposed

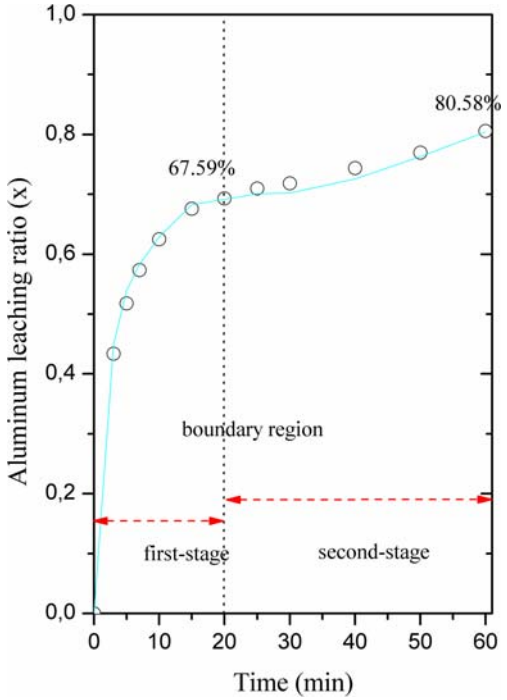

Fig. 7 Division of stages in Al leaching process

regions of leaching rate as shown in Fig. 7. The exponential rate ($t < 20$ min) is used in the first stage and the linear rate ($t > 20$ min) in the second stage. The mechanisms of leaching process were further assessed separately for each stage and the integration limits of the corresponding differential mass balance equation consequently changed. For the first-stage process, Eqs. (2) and (3) were applied for surface chemical reaction and product-layer diffusion, respectively. For the second stage, the equation based on surface chemical reaction as rate of limiting step led to:

$$\frac{t-t_1}{\tau_c} = 1-\left(\frac{1-x}{1-x_1}\right)^{1/3} \tag{4}$$

$$\tau_c = \rho_B R(1-x_1)^{1/3}/bM_w k_c C_A \tag{5}$$

where t is the total reaction time, t_1 is the first-stage reaction time, x is the total Al leached out, and x_1 is the Al leached out in the first stage. Both t_1 and x_1 values were obtained from experimental data as the initial conditions. The kinetic equation for the rate-limiting step based on product-layer diffusion can be further expressed as follows:

$$\frac{t-t_1}{\tau_i} = 1-3\left(\frac{1-x}{1-x_1}\right)^{2/3} + 2\frac{(1-x)}{(1-x_1)} \tag{6}$$

$$\tau_i = \rho_B R^2(1-x_1)^{2/3}/6bM_w D_e C_A. \tag{7}$$

Table 2 shows the constants of leaching rate in the first and second stages of various HCl concentrations. It was clear that in the first stage, the leaching process of Al was controlled by the product-layer diffusion since the correlation coefficient value (R^2) for the rate constant of product-layer diffusion (K_i) was higher than that of surface chemical reaction (K_c). For the second-stage process, it was found that the R^2 value of K_c was slightly higher than that of K_i especially at a higher acid concentration (> 1 M). This finding implies that Al leaching could be appropriately controlled by chemical reaction. A similar finding was observed at various particle sizes for both first and second stages as presented in Table 3; furthermore, the R^2 value of K_i for second stage was very low, hence, the diffusion could not be justified to control the process. This revealed that the diffusion process was dominant at the beginning of process for a short time. Hence, at the second stage, after the particle experienced the shrinkage by time, the diffusion rate would be very fast, and the chemical reaction subsequently became the rate-limiting step. Furthermore, the leaching rate process depends more on the particle size compared to acid concentration as the increase in rate constants became twofold when the particle size was reduced from 120 to 200 to 200–325 mesh.

The division of two stages was also clearly observed at the temperature effect with significantly different values of R^2 for both product-layer diffusion and chemical reaction as shown in Table 4. It was reported that at a lower temperature, the

Table 2 Parameters of the kinetic model for Al leaching at different acid concentrations

Acid concentration (M)	First-stage of leaching process				Second-stage of leaching process			
	Rate constants (min^{-1})		Correlation coefficient (R^2)		Rate constants (min^{-1})		Correlation coefficient (R^2)	
	K_i	K_c	R^2_i	R^2_c	K_i	K_c	R^2_i	R^2_c
6	0.0212	0.0293	0.72	0.39	0.0006	0.0025	0.93	0.98
4	0.0190	0.0274	0.85	0.56	0.0006	0.0025	0.95	0.96
2	0.0153	0.0242	0.93	0.67	0.0007	0.0027	0.93	0.99
1	0.0113	0.0204	0.94	0.74	0.0008	0.003	0.96	0.92

Table 3 Parameters of the kinetic model for Al leaching at different particle sizes

Particle size (mesh)	First-stage of leaching process				Second-stage of leaching process			
	Rate constants (min^{-1})		Correlation coefficient (R^2)		Rate constants (min^{-1})		Correlation coefficient (R^2)	
	K_i	K_c	${R^2}_i$	${R^2}_c$	K_i	K_c	${R^2}_i$	${R^2}_c$
+ 200/− 325	0.0179	0.0265	0.89	0.57	0.0010	0.0033	0.80	0.98
+ 120/− 200	0.0164	0.0164	0.97	0.91	0.0003	0.0018	0.95	0.97
+ 70/− 120	0.0048	0.0125	0.93	0.96	0.0003	0.0018	0.93	0.97

chemical reaction control was more appropriate; conversely at higher temperature, the leaching process was controlled by product-layer diffusion (Cui et al. 2015). In this study, the R^2 values were similar for both, the chemical reaction and layer diffusion, at 30 °C in the first stage; the kinetic model of product-layer diffusion fitted well at a higher temperature. In the second stage, the chemical reaction was dominantly observed to be the rate-limiting step. It indicated that temperature contributed significantly to the leaching process; in as much as the constant rate can be related to the exponential function of temperature by Arrhenius equation: $K = A\, e^{\left(-\frac{Ea}{R\,T}\right)}$. A is the pre-exponential factor; E_a is the activation energy (kJ mol^{-1}); R is the gas constant, 8.314×10^{-3} kJ mol^{-1} K^{-1}, and T is the temperature (K).

The activation energies obtained in this work for the first stage and second stage were 9.58 kJ/mol and 10.73 kJ/mol, respectively. Compared with other results (Table 5), the value of activation energy obtained in the current study was lower than that in those literatures (Cheng et al. 2012; Cui et al. 2015; Tang et al. 2010). It implies that the leaching process of aluminum from WTS using HCl was easier. It was reported (Tang et al. 2010) that dissolution kinetics controlled by surface chemical reaction resulted in a higher activation energy (> 42 kJ/mol), whereas a lower activation energy (< 20 kJ/mol) suggested that product-layer diffusion is the rate-controlling step (Cui et al. 2015). The value of activation energy for first stage in this work was in agreement to those reported; however, the activation energy value in second stage was out of range for chemical reaction as the rate-limiting step. It is possible since they only evaluated the leaching process in the first stage, while a further way of the second stage was also observed in this work as the continual process. Hence, due to shrinkage phenomenon that diminishes the diffusion barrier, the chemically controlled process in the second stage would be more plausible to take place thus implying the low activation energy.

To prove the involvement of a series-kinetic control process of chemical reaction and product-layer diffusion, a combined kinetic model was proposed. The combined kinetic model is described as follows:

$$K_p t = \alpha\left[1-(1-x)^{1/3}\right] + (1-\alpha)\left[1-3(1-x)^{2/3} + 2(1-x)\right] \quad (8)$$

$$K_{pm}(t-t_1) = \alpha\left[1-3\left(\frac{1-x}{1-x_1}\right)^{2/3} + 2\frac{(1-x)}{(1-x_1)}\right] + (1-\alpha)\left[1-\left(\frac{1-x}{1-x_1}\right)^{1/3}\right] \quad (9)$$

$$\alpha = \frac{K_i}{K_c}. \quad (10)$$

K_p is the rate constant of the combined kinetic model. Equations 8 and 9 were applied for the first- and second-stage process, respectively. α is the ratio of K_i (coefficient for diffusion rate) to K_c (coefficient for chemical reaction rate).

Table 4 Parameters of the kinetic model for Al leaching at various temperatures

Temperature (°C)	First-stage of leaching process				Second-stage of leaching process			
	Rate constants (min^{-1})		Correlation coefficient (R^2)		Rate constants (min^{-1})		Correlation coefficient (R^2)	
	K_i	K_c	${R^2}_i$	${R^2}_c$	K_i	K_c	${R^2}_i$	${R^2}_c$
90	0.0179	0.0265	0.89	0.57	0.0010	0.0033	0.81	0.98
70	0.0128	0.0220	0.87	0.60	0.0002	0.0015	0.74	0.95
50	0.0100	0.0190	0.95	0.79	0.0002	0.0015	0.73	0.94
30	0.0068	0.0150	0.93	0.95	0.0002	0.0120	0.71	0.92

Table 5 Activation energy comparison of leaching process from literature

Time min	Temperature °C	Model	Rate-controlling step	Activation energy (kJ/mol)	Raw material	Solvent	Ref.
0–160	60–100	One stage	Surface chemical reaction	43	Kaolin residue	Hydrochloric acid	Tang et al. (2010)
			Diffusion process	24			
0–60	10–70	One stage	Inert-layer diffusion	32.32	Water purification sludge	Sulfuric acid	Cheng et al. (2012)
0–120	40–80	One-stage	Surface reaction	57.65	Coal mining waste	Hydrochloric acid	Cui et al. (2015)
	90–106		Product-layer diffusion	12.33			
0–15	30–90	First stage	Product-layer diffusion	9.58	Waste treatment sludge	Hydrochloric acid	Present study
15–60		Second stage	Surface chemical reaction	10.73			

The higher value of α implies chemical reaction rate is controlling. The value of α is in the range of 0–1.

Figures 8a and b show the plot of the combined kinetic model for first and second stages at the temperature of 70 °C, respectively. The figures for other temperatures (not presented here) show similar trends as shown in Fig. 8. In Fig. 8a, the lower value of α led to higher value of R^2; it means that the product-layer diffusion controlled the process rate. This finding thus confirms the previous conclusion that in the first stage, the leaching process was predominantly controlled by product-layer diffusion. In the second stage, the kinetic model with the high value of α fitted well the data as indicated by high value of R^2. Hence, the leaching mechanism was mainly affected by a chemical reaction process. The proposed model was validated by using data from literature (Yang et al. 2019b), where the aluminum removal from diamond wire saw powder using hydrochloric acid 2 M at 60 °C was carried out. As shown in Fig. 9, good correlation fittings in the first stage ($R^2 = 0.92$) and the second stage ($R^2 = 0.98$) that describes the product-layer controlled diffusion and the chemical reaction controlled, respectively, were obtained. This finding obviously disproves the previous conclusion (Yang et al. 2019b) regarding the failed mathematical approach at higher temperature ($R^2 = 0.43$–0.70) due to finer particle. This again confirms the previous finding using the separated model. Thus, the new combined kinetic model based on the general shrinkage core model could be well proposed for the system of leaching or extraction process. Moreover, the proposed model can be applied in other applications such as dehydration reaction, hydration kinetic, hydrolysis process, and pyrolysis

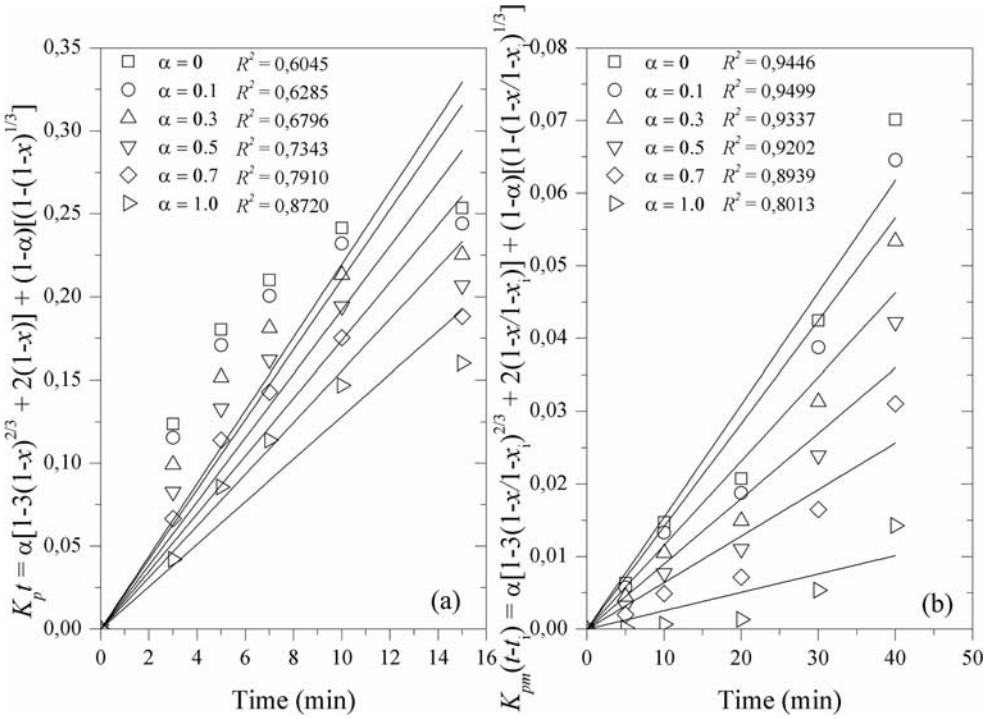

Fig. 8 Profile of the combined kinetic model against experimental data at 70 °C for **a** first-stage leaching and **b** second-stage leaching

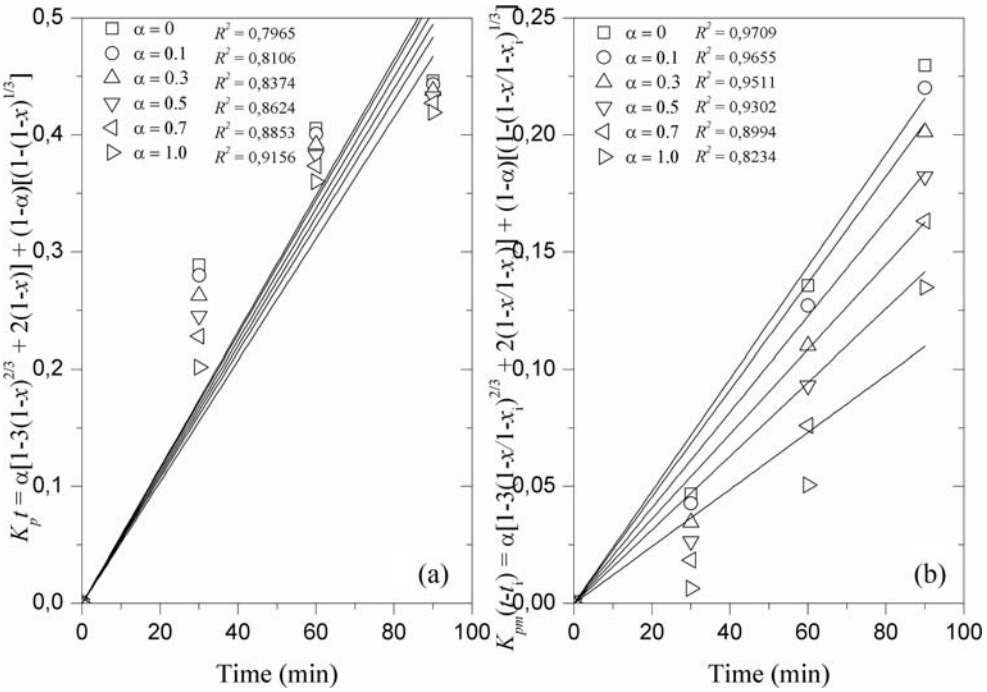

Fig. 9 Validated profile of the combined kinetic model against experimental data from literature for **a** first-stage leaching and) second-stage leaching

process to predict the experimental data as the rate of shrinkage was shown by exponential and linear curves (Farsi et al. 2019; Huang et al. 2018; Lan et al. 2015; Zhang et al. 2019).

For future step, the Al produced through leaching process could be precipitated using a base to form $AlPO_4$; this could be applied in phosphate industry or fertilizer in agriculture (Muisa et al. 2020; Pradel et al. 2020). On other hand, the Alum sludge can be used as absorbent for heavy metals (Dassanayake et al. 2015). After extraction process using HCl, the non-toxic organic materials remain in the sludge (Smith et al. 2009). This residual sludge essentially provides geopolymeric feedstock (Gomes et al. 2019). Furthermore, the residue becomes secondary raw material for the ceramic and glass industries (Zichella et al. 2020).

Conclusions

The kinetics of Al leaching from WTS was investigated using HCl. Leaching experiments were performed with four different acid concentrations, three different particle sizes, and four different temperatures. Al leaching efficiency increased as HCl concentration changed from 1 to 4 M. However, the limited solubility of $AlCl_3$ at higher concentration (6 M) hindered the leaching reaction. In addition, both smaller particle size and higher temperature resulted in higher leaching efficiency. The proposed kinetic model revealed the importance of the dividing the leaching process into two stages. The first stage was more suitable for the kinetic of product-layer diffusion, while the second stage was controlled by the chemical reaction. The proposed model that has been well validated with the literature data showed the prominence to be developed for wide application process using shrinking model.

Acknowledgments The first author is grateful for Sandwich-Like Program from the Directorate General of Science & Technology Resource and Higher Education (DGSTRHE), Republic of Indonesia in collaboration with National Taiwan University of Science and Technology (Taiwan Tech) Taiwan.

Funding information This study was financially supported by the Directorate General of Higher Education, Ministry of Education and Culture, Republic of Indonesia.

Compliance with ethical standards

Conflict of interest The authors declare that there is no conflict of interest.

References

Adekola FA, Baba AA, Girigisu S (2017) Dissolution kinetics of kaolin mineral in acidic media for predicting optimal condition for alum production. J Cent S Univ 24(2):318–324

Ahmad T, Ahmad K, Alam M (2016a) Characterization of water treatment plant's sludge and its safe disposal options. Procedia Environ Sci 35:950–955

Ahmad T, Ahmad K, Alam M (2016b) Sustainable management of water treatment sludge through 3'R' concept. J Clean Prod 124:1–13

Ajeel SA, Waadulah HM, Sultan DA (2012) Effects of H_2SO_4 and HCl concentration on the corrosion resistance of protected low carbon steel. Al-Rafdain Eng J 20(6):70–76

Baba AA, Adekola AF, Bale RB (2009) Development of a combined pyro- and hydro-metallurgical route to treat spent zinc–carbon batteries. J Hazard Mater 171(1):838–844

Babatunde AO, Zhao YQ (2007) Constructive approaches toward water treatment works sludge management: an international review of beneficial reuses. Crit Rev Environ Sci Technol 37(2):129–164

Bhattacharyya S, Behera PS (2017) Synthesis and characterization of nano-sized α-alumina powder from kaolin by acid leaching process. Appl Clay Sci 146:286–290

Brantley S, Kubicki J, White A (2008) Kinetics of water-rock interaction. Springer-Verlag, New York

Cheng W-P, Fu C-H, Chen P-H, Yu R-F (2012) Dynamics of aluminum leaching from water purification sludge. J Hazard Mater 217-218: 149–155

Cheng W-P, Chen P-H, Yu R-F, Ho W-N (2016) Treating ammonium-rich wastewater with sludge from water treatment plant to produce ammonium alum. Sust Environ Res 26(2):63–69

Cui L, Guo Y, Wang X, Du Z, Cheng F (2015) Dissolution kinetics of aluminum and iron from coal mining waste by hydrochloric acid. Chin J Chem Eng 23(3):590–596

Dassanayake KB, Jayasinghe GY, Surapaneni A, Hetherington C (2015) A review on alum sludge reuse with special reference to agricultural applications and future challenges. Waste Manag 38:321–335

Farsi A, Kayhan Ö, Zamfirescu C, Dincer I, Naterer GF (2019) Kinetic and hydrodynamic analyses of chemically reacting gas-particle flow in cupric chloride hydrolysis for the Cu-Cl cycle. Int J Hydrog Energy 44(49):26783–26793

Gomes SDC, Zhou JL, Li W, Long G (2019) Progress in manufacture and properties of construction materials incorporating water treatment sludge: a review. Resour Conserv Recy 145:148–159

Hagen Mvd, Järnberg J. (2009). The Nordic expert group for criteria documentation of health risks from chemicals. In: Arbete och Hälsa, Vol. 43, Göteborgs Universitet. Göteborg, pp. 1–123

Haynes RJ, Zhou Y-F (2015) Use of alum water treatment sludge to stabilize C and immobilize P and metals in composts. Environ Sci Pollut Res 22(18):13903–13914

Huang Y, Zhang M, Lyu J, Yang H, Liu Q (2018) Modeling study on effects of intraparticle mass transfer and secondary reactions on oil shale pyrolysis. Fuel 221:240–248

Jiménez B, Martínez M, Vaca M (2007) Alum recovery and wastewater sludge stabilization with sulfuric acid. Water Sci Technol 56(8):133–141

Keeley J, Jarvis P, Smith AD, Judd SJ (2016) Coagulant recovery and reuse for drinking water treatment. Water Res 88:502–509

Lan S, Zondag H, van Steenhoven A, Rindt C (2015) Kinetic study of the dehydration reaction of lithium sulfate monohydrate crystals using microscopy and modeling. Thermochim Acta 621:44–55

Meng Z, Zhou Z, Zheng D, Liu L, Dong J, Yang Y, Li X, Zhang T (2018) Optimizing dewaterability of drinking water treatment sludge by ultrasound treatment: correlations to sludge physicochemical properties. Ultrason Sonochem 45:95–105

Muisa N, Nhapi I, Ruziwa W, Manyuchi MM (2020) Utilization of alum sludge as adsorbent for phosphorus removal in municipal wastewater: a review. J Water Process Eng 35:101187

Nair AT, Ahammed MM (2014) Coagulant recovery from water treatment plant sludge and reuse in post-treatment of UASB reactor effluent treating municipal wastewater. Environ Sci Pollut Res 21(17): 10407–10418

Nair AT, Ahammed MM (2015) The reuse of water treatment sludge as a coagulant for post-treatment of UASB reactor treating urban wastewater. J Clean Prod 96:272–281

Okuda T, Nishijima W, Sugimoto M, Saka N, Nakai S, Tanabe K, Ito J, Takenaka K, Okada M (2014) Removal of coagulant aluminum from water treatment residuals by acid. Water Res 60:75–81

Ooi TY, Yong EL, Din MFM, Rezania S, Aminudin E, Chelliapan S, Abdul Rahman A, Park J (2018) Optimization of aluminium recovery from water treatment sludge using response surface methodology. J Environ Manag 228:13–19

Pradel M, Lippi M, Daumer M-L, Aissani L (2020) Environmental performances of production and land application of sludge-based phosphate fertilizers—a life cycle assessment case study. Environ Sci Pollut Res 27(2):2054–2070

Raza N, Zafar ZI, Najamul H, Kumar RV (2015) Leaching of natural magnesite ore in succinic acid solutions. Int J Miner Process 139: 25–30

Seidel A, Zimmels Y (1998) Mechanism and kinetics of aluminum and iron leaching from coal fly ash by sulfuric acid. Chem Eng Sci 53(22):3835–3852

Shalchian H, Khaki JV, Babakhani A, Michelis ID, Veglio F, Parizi MT (2018) An enhanced dissolution rate of molybdenite and variable activation energy. Hydrometallurgy 175:52–63

Smith KM, Fowler GD, Pullket S, Graham NJD (2009) Sewage sludge-based adsorbents: a review of their production, properties and use in water treatment applications. Water Res 43(10):2569–2594

Tang A, Su L, Li C, Wei W (2010) Effect of mechanical activation on acid-leaching of kaolin residue. Appl Clay Sci 48(3):296–299

Tian C, Lu H, Wei K, Ma W, Xie K, Wu J, Lei Y, Yang B, Morita K (2018) Effect of CH_3COOH on hydrometallurgical purification of metallurgical-grade silicon using HCl-HF leaching. JOM J Miner Met Mater Soc 70(4):527–532

Xu GR, Yan ZC, Wang YC, Wang N (2009) Recycle of alum recovered from water treatment sludge in chemically enhanced primary treatment. J Hazard Mater 161(2):663–669

Yang Q, Li Q, Zhang G, Shi Q, Feng H (2019a) Investigation of leaching kinetics of aluminum extraction from secondary aluminum dross with use of hydrochloric acid. Hydrometallurgy 187:158–167

Yang S, Wei K, Ma W, Xie K, Wu J, Lei Y (2019b) Kinetic mechanism of aluminum removal from diamond wire saw powder in HCl solution. J Hazard Mater 368:1–9

Yang S, Wan X, Wei K, Ma W, Wang Z (2020) Dissolution and mineralization behavior of metallic impurity content in diamond wire saw silicon powder during acid leaching. J Clean Prod 248:119256

Zhang Y, Bouillon C, Vlasopoulos N, Chen JJ (2019) Measuring and modeling hydration kinetics of well cements under elevated temperature and pressure using chemical shrinkage test method. Cem Concr Res 123:105768

Zichella L, Dino GA, Bellopede R, Marini P, Padoan E, Passarella I (2020) Environmental impacts, management and potential recovery of residual sludge from the stone industry: the piedmont case. Resour Policy 65:101562